JGR Atmospheres

RESEARCH ARTICLE
10.1029/2023JD038474

Understanding the Mechanisms for Tropical Surface Impacts of the Quasi-Biennial Oscillation (QBO)

Jorge L. García-Franco[1,2], Lesley J. Gray[1,3], Scott Osprey[1,3], Aleena M. Jaison[1], Robin Chadwick[4,5], and Jonathan Lin[2]

[1]Atmospheric, Oceanic and Planetary Physics, University of Oxford, Oxford, UK, [2]Lamont-Doherty Earth Observatory, Columbia University, New York, NY, USA, [3]National Centre for Atmospheric Science, Oxford, UK, [4]Met Office Hadley Centre, Exeter, UK, [5]Department of Mathematics, Global Systems Institute, University of Exeter, Exeter, UK

Abstract The impact of the quasi-biennial oscillation (QBO) on tropical convection and precipitation is investigated through nudging experiments using the UK Met Office Hadley Center Unified Model. The model control simulations show robust links between the internally generated QBO and tropical precipitation and circulation. The model zonal wind in the tropical stratosphere was nudged above 90 hPa in atmosphere-only and coupled ocean-atmosphere configurations. The convection and precipitation in the atmosphere-only simulations do not differ between the experiments with and without nudging, which may indicate that SST-convection coupling is needed for any QBO influence on the tropical lower troposphere and surface. In the coupled experiments, the precipitation and sea-surface temperature relationships with the QBO phase disappear when nudging is applied. Imposing a realistic QBO-driven static stability anomaly in the upper-troposphere lower-stratosphere is not sufficient to simulate tropical surface impacts. The nudging reduced the influence of the lower troposphere on the upper branch of the Walker circulation, irrespective of the QBO, indicating that the upper tropospheric zonal circulation has been decoupled from the surface by the nudging. These results suggest that grid-point nudging mutes relevant feedback processes occurring at the tropopause level, including high cloud radiative effects and wave mean flow interactions, which may play a key role in stratospheric-tropospheric coupling.

Plain Language Summary The interaction between the stratosphere and the troposphere is well known to produce surface impacts in the extratropics. However, whether stratosphere-troposphere interactions affect the surface in the tropics associated with the variability of the stratospheric quasi-biennial oscillation (QBO) is yet to be determined because the observational record is too short and tropical tropospheric variability masks any potential signal of the stratosphere. In this paper, we examine hypotheses that explain how the QBO could affect tropical deep convection and tropical precipitation variability through targeted model experiments which prescribe the equatorial stratosphere. Our results indicate that prescribing the zonal wind in the stratosphere remove links between surface precipitation and the QBO. Therefore, nudging the stratosphere decouples the stratospheric mean flow and anomalies from the tropospheric processes, which emphasizes the role of feedbacks.

Key Points:

- Nudging the stratospheric quasi-biennial oscillation (QBO) removes impacts to tropical precipitation
- The QBO impact on upper-level static stability is not sufficient to influence tropical precipitation in this model
- Feedbacks, muted by nudging, may be key for stratospheric-tropospheric coupling

Supporting Information:

Supporting Information may be found in the online version of this article.

Correspondence to:

S. Osprey,
s.osprey@physics.ox.ac.uk

Citation:

García-Franco, J. L., Gray, L. J., Osprey, S., Jaison, A. M., Chadwick, R., & Lin, J. (2023). Understanding the mechanisms for tropical surface impacts of the quasi-biennial oscillation (QBO). *Journal of Geophysical Research: Atmospheres*, *128*, e2023JD038474. https://doi.org/10.1029/2023JD038474

Received 1 JAN 2023
Accepted 16 JUN 2023

Author Contributions:

Conceptualization: Jorge L. García-Franco, Lesley J. Gray, Scott Osprey, Robin Chadwick
Formal analysis: Jorge L. García-Franco, Aleena M. Jaison, Jonathan Lin
Investigation: Jorge L. García-Franco, Lesley J. Gray
Methodology: Jorge L. García-Franco, Lesley J. Gray, Scott Osprey, Aleena M. Jaison
Software: Jorge L. García-Franco
Supervision: Lesley J. Gray, Scott Osprey, Robin Chadwick
Visualization: Jorge L. García-Franco

1. Introduction

The stratospheric quasi-biennial oscillation (QBO) has been linked to tropical deep convection for several decades (Collimore et al., 2003; Giorgetta et al., 1999; W. M. Gray, 1984; Hitchman et al., 2021; Liess & Geller, 2012). Observations show that the magnitude and location of tropical precipitation as well as several cloud properties are statistically related to the QBO phase (García-Franco et al., 2022; L. J. Gray et al., 2018; Liess & Geller, 2012; Sweeney et al., 2023; Tseng & Fu, 2017). However, the extent to which the tropical troposphere and stratosphere are coupled, as well as the mechanisms that connect these two layers, remain a matter of debate for several reasons (Haynes et al., 2021; Hitchman et al., 2021; Martin, Son, et al., 2021).

First, the observational record is relatively short to disentangle any effect of the QBO on tropical convection from the strong influence of El Niño-Southern Oscillation (ENSO), which is the dominant driver of tropical variability on interannual timescales (García-Franco et al., 2020, 2022; Hu et al., 2012). ENSO influences the QBO, for example, its descent rate and amplitude through its modulation of the tropical waves that generate the QBO (Geller et al., 2016; Schirber, 2015; Taguchi, 2010). Figure 1 shows the QBO W-E composite difference in

Writing – original draft: Jorge L. García-Franco, Lesley J. Gray, Robin Chadwick, Jonathan Lin
Writing – review & editing: Jorge L. García-Franco, Lesley J. Gray, Scott Osprey, Jonathan Lin

the observed (1979–2021) sea-surface temperature (SST) record which resembles an El Niño-like pattern due to the observed aliasing between the QBO and ENSO in recent decades (Domeisen et al., 2019; García-Franco et al., 2022). For these reasons, the attribution of anomalies in the tropics to the QBO usually requires the removal of the ENSO signal through linear regression (L. J. Gray et al., 2018; J.-H. Lee et al., 2019; Liess & Geller, 2012; Sweeney et al., 2023).

Second, there is no clear understanding of how the QBO could modulate tropical deep convection. Several hypotheses have been proposed to explain a coupling of the QBO and the tropical troposphere which involve static stability (e.g., Haynes et al., 2021; Nie & Sobel, 2015), vertical wind shear (e.g., W. M. Gray et al., 1992), a QBO-Walker circulation feedback (e.g., García-Franco et al., 2022; Hitchman et al., 2021; Yasunari, 1989) and cloud feedbacks (Sakaeda et al., 2020). However, there is no clear understanding which of these hypotheses, if any, is the primary mechanism for a downward impact from the QBO on tropical convection.

The static stability hypothesis suggests that induced meridional circulation driven by the descending QBO shear impacts the static stability in the region of the upper troposphere-lower stratosphere (UTLS; Back et al., 2020; Collimore et al., 2003; Giorgetta et al., 1999; W. M. Gray et al., 1992; Liess & Geller, 2012; Nie & Sobel, 2015). This hypothesis suggests that decreased UTLS static stability, found under the easterly phase (QBOE) compared to the westerly phase (QBOW), leads to enhanced convection under QBOE (Collimore et al., 2003) which could also explain, for example, the stronger convection associated with the Madden–Julian Oscillation under QBOE conditions (Back et al., 2020; Hendon & Abhik, 2018; Son et al., 2017; Yoo & Son, 2016).

Observational and modeling results indicate that the QBO impact in the tropics is not zonally symmetric (Collimore et al., 2003; García-Franco et al., 2022; Liess & Geller, 2012). For this reason, several studies have suggested an interaction between the QBO and the Walker circulation (Hitchman et al., 2021; Hu et al., 2012; Liess & Geller, 2012; Yasunari, 1989). Observations show that the Walker circulation was weaker under QBOW compared to QBOE in the period of 1979–2021 (García-Franco et al., 2022; Hitchman et al., 2021) but the causal direction of this relationship remains to be well understood.

Cloud-radiative effects (CREs) associated with the variability of tropical upper-level clouds have been proposed to explain the QBO-MJO link (Lim & Son, 2022; Lin & Emanuel, 2023; Martin, Son, et al., 2021; Sakaeda et al., 2020; Sun et al., 2019). It is also plausible that high cloud variability explains the QBO tropical surface impacts more generally. For instance, observations show that the QBO is strongly linked to the interannual variability of upper-level clouds in the tropical tropopause layer (TTL; Davis et al., 2013; Liess & Geller, 2012; Tegtmeier et al., 2020; Tseng & Fu, 2017), with higher cloud fraction observed under QBOE compared to QBOW (Davis et al., 2013; Sweeney et al., 2023; Zhang & Zhang, 2018). One possible mechanism is that a QBO modulation of the mean state of cloud fraction affects the stability of the UTLS. In particular, more clouds under QBOE could lead to a radiative cooling of the stratosphere and warming of the upper troposphere (Hartmann et al., 2001), which would destabilize the upper troposphere (Hong et al., 2016; Needham & Randall, 2021).

A second potential mechanism involves cloud radiative feedbacks (Lin & Emanuel, 2023; Sakaeda et al., 2020). If convection is more efficient at producing high clouds under QBOE, either through a thermodynamic modulation of tropopause temperatures (Sakaeda et al., 2020) or dynamically due to upward wave propagation interacting with the stratospheric mean flow (Lin & Emanuel, 2023), then, when convection occurs anomalous high cloud coverage would lead to CREs (Hartmann & Berry, 2017). The high cloud radiative feedbacks can change the buoyancy of ascending parcels (Allan, 2011; Harrop & Hartmann, 2016; Hartmann & Berry, 2017; Rädel et al., 2016). Both mechanisms would result in increased convective activity and precipitation under QBOE compared to QBOW.

Since observations and theory have not successfully identified the mechanism for QBO tropical teleconnections, several studies have turned to numerical models such as cloud-resolving models (CRMs; Back et al., 2020; Martin et al., 2019; Nie & Sobel, 2015) and General Circulation Models (GCMs; H. Kim et al., 2020; J. C. K. Lee & Klingaman, 2018; Serva et al., 2022) to identify pathways of stratospheric-tropospheric coupling. Although GCMs are more comprehensive than CRMs, stratospheric and tropospheric biases have hindered the potential use of these models to tackle this problem. For example, GCMs underestimate the amplitude of the QBO in the lowermost stratosphere (Figure S1 in Supporting Information S1 and H. Kim et al., 2020; J. C. K. Lee & Klingaman, 2018; Martin, Orbe, et al., 2021) which means that the variability of the UTLS static stability associated with the QBO is lower than observed (Bushell et al., 2020; J. C. K. Lee & Klingaman, 2018; Rao et al., 2020; Richter et al., 2020; Schenzinger et al., 2017).

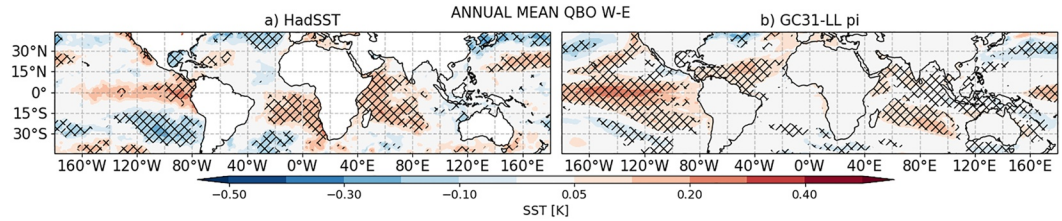

Figure 1. Annual mean sea-surface temperature (SST) [K] QBO W-E differences in (a) HadSST data set and (b) the pre-industrial control simulation of the Unified Model GC31-LL pi. Hatching denotes significance to the 95% confidence level.

The weak QBO amplitude bias in the lower stratosphere (Figure S1 in Supporting Information S1) has been hypothesized to explain why some observed teleconnections, including the MJO-QBO relationship, are not diagnosed in GCMs (H. Kim et al., 2020; J. C. K. Lee & Klingaman, 2018; Martin, Orbe, et al., 2021). Due to these biases, several studies have performed or suggested experiments in which the model stratosphere is relaxed toward an observed or idealized state of the stratosphere, also known as nudging (e.g., Garfinkel & Hartmann, 2011; J. C. K. Lee & Klingaman, 2018; Martin, Orbe, et al., 2021; Richter et al., 2020). The nudging technique can help remove biases, identify causal pathways and test specific hypotheses to understand mechanisms (L. Gray et al., 2020; Haynes et al., 2021; Politowicz & Hitchman, 1997).

This study aims to understand QBO tropical teleconnections by addressing the issue of QBO model biases using experiments with stratospheric nudging of the Met Office Hadley Center (MOHC) Unified Model (UM). The UM is a state-of-the-art GCM that is able to simulate an internally generated QBO that is reasonably similar to observations, except for the weak amplitude bias in the lower stratosphere (Richter et al., 2020). The UM exhibits robust signals of the QBO in the tropical troposphere (García-Franco et al., 2022), including an SST signal (see Figure 1) that is similar to the observed record. In addition, nudging has previously been successfully applied in this model (L. Gray et al., 2020; Telford et al., 2008).

The main purpose of this study is to evaluate the effect of nudging on the representation of tropical surface impacts of the QBO. The results of these experiments are used to critically examine several of the existing hypotheses suggested to explain QBO-convection links: the static stability mechanism, QBO-Walker circulation relationships, and the role of high clouds. The paper is presented as follows. Section 2 describes the nudging experiments and datasets used to inform the experimental results. Section 3 presents the results of the experiments. The final section presents a discussion and conclusions that can be drawn from this study.

2. Model, Methodology and Data

2.1. The Met Office Unified Model

The MOHC UM uses a seamless modeling framework that allows the setup of simulations using various configurations; for example, various horizontal resolutions can be used while maintaining the same parametrizations and dynamical core (Walters et al., 2019). The version of the UM used in this study employs the Global Coupled (GC) configuration 3.1 (GC3.1; Walters et al., 2019; Williams et al., 2018). The model is run in both atmosphere-only (AMIP) and in coupled ocean-atmosphere mode. The model has 85 atmospheric levels, 4 soil levels and 75 ocean levels with a model top at 0.4 hPa (approximately 85 km; Walters et al., 2019). All experiments, both AMIP and coupled, were run at N96 atmospheric horizontal resolution (1.875° latitude × 1.25° longitude). The coupled experiments use an oceanic resolution of 0.25° (ORCA025) using the NEMO model (Storkey et al., 2018). The model includes a self-generated QBO via a non-orographic gravity wave scheme (Bushell et al., 2015; Walters et al., 2019) that compares well with the observed QBO (Richter et al., 2020).

2.2. Nudging Scheme

Nudging refers to the relaxation of a model variable toward a specified state, which can be taken from reanalysis, observations or idealized states (L. Gray et al., 2020; Martin, Orbe, et al., 2021). In the UM setup, three variables can be nudged: air temperature (T) and the zonal (u) and meridional (v) components of the wind; in this study

we use ERA5 as the nudging data. The relaxation is applied at each grid-point, in contrast to other studies (e.g., Martin, Orbe, et al., 2021) that employ a spectral model and apply the relaxation only to the zonal-mean component. Specifically, the UM uses a Newtonian relaxation technique (L. Gray et al., 2020; Telford et al., 2008) which sets the field to be nudged (F) at each time-step through the following equation:

$$\Delta F = G\Delta t(F_{ndg} - F_{model}), \tag{1}$$

where ΔF is the discrete change of F at each time-step, G is the relaxation parameter, Δt is the time interval [h], F_{ndg} is the value of the field from the nudging data and F_{model} is the model value of the field at the last time-step (Telford et al., 2008).

The relaxation parameter G sets the strength of the nudging and is linked with the relaxation timescale (τ) by $G = 1/\tau$. Previous studies (L. Gray et al., 2020; Telford et al., 2008) have shown that a 6-hr relaxation time-scale is sufficient to constrain the stratosphere in the model and so the same parameter was used for our simulations ($G = \frac{1}{6}\,\mathrm{h}^{-1}$).

In all experiments, nudging is applied at all longitudes and at full strength within the latitude band of 10°S–10°N, with a linear tapering of 10° so that $G = 0$ poleward of 20N and 20S. The nudging is applied at full strength between 10 and 70 hPa (model levels 50–72) with a linear tapering of four model levels above and below this range so that $G = 0$ at all heights below 90 hPa and above 4 hPa. The lowermost level of nudging is above the maximum of UTLS cloud fraction (Lin & Emanuel, 2023), however, observations show a QBO influence on UTLS clouds within our nudging domain, extending from 15 to 19 km (Sweeney et al., 2023).

2.3. Experimental Design

All experiments, both AMIP and coupled, use a present-day climate configuration where all external forcings are set constant to those of the year 2000. Atmosphere-only (AMIP) experiments are performed to examine whether the QBO modifies tropical deep convection and precipitation under prescribed SSTs or whether SST feedbacks are necessary for QBO-tropical connections. Three sets of AMIP experiments were run: Control, Nudged and Shifted. For each experiment, a three-member ensemble of the AMIP simulations were performed for 32 years (1981–2012) using prescribed SST and sea-ice for the period 1981–2012 provided in the AMIP forcing specification of the CMIP6 project. In the control experiment, the model stratosphere was free to evolve. In the Nudged experiment, the equatorial zonal wind was nudged, as described in the previous section, toward ERA5 nudging data corresponding with the same years as the SST data.

The Shifted experiment was run to check whether any QBO responses found in the troposphere arose solely as a result of the imposed QBO winds or whether they also relied on an in-phase relationship with the imposed SSTs (which also contain a QBO signal, as shown in Figure 1a). In the shifted experiment, the nudging data was shifted by 1 year with respect to the SSTs. Thus, the model year 1997 was run using 1997 SSTs but zonal winds in the stratosphere were those of 1996, so that any QBO signal in the imposed SST field did not align with the QBO signal in the atmosphere. An alternative approach would be to *shuffle* the SSTs so that each year is run with randomly selected SSTs. However, since we are performing multi-year simulations shuffling has associated issues of how to join the randomly-selected SSTs at the year-boundary to form a coherent multi-year SST time-series. To avoid this issue we decided to simply shift the zonal wind nudging data by 1 year so the QBO phase and SSTs were not aligned.

Coupled ocean-atmosphere experiments are performed to diagnose potential SST-convection relationships with the QBO. A six-member control ensemble and a six-member nudged ensemble were run for 35 years (1981–2015 model years). Each ensemble member was initialized from different ocean/atmosphere initial conditions, in order to decrease the role that internal variability may have on these simulations. Specifically, the coupled ocean-atmosphere configuration was initialized using oceanic conditions from a 100-year simulation of the same model configuration that were taken 10 years apart from each other.

In addition to the main experiments described above, which are relatively short, a 500-year coupled ocean-atmosphere CMIP6 pre-industrial control simulation (Figure 1b) is used to assess internal variability. This CMIP6 simulation uses the same model set-up but with constant external forcing at pre-industrial levels (Menary et al., 2018). A summary of the experiments is given in Table 1.

Table 1
Experimental Setup Indicating the Model Configuration, the Period, Number of Ensemble Members (Ens.) and Relaxation Details

Name	Configuration	Period	Ens.	Nudging
AMIP	Atmosphere-only	1981–2012	3	ERA5
AMIP-Control	Atmosphere-only	1981–2012	3	No nudging
AMIP-Shifted	Atmosphere-only	1981–2012	3	ERA5 Relaxation shifted—1 year
Coupled Nudged	Coupled ocean-atmosphere	1981–2015	6	ERA5
Coupled Control	Coupled ocean-atmosphere	1981–2015	6	No nudging

2.4. Indices and Analysis Methods

Composite and regression analysis are used to evaluate the differences amongst experiments, as in García-Franco et al. (2022). ENSO is measured through the standard Oceanic Niño Index, that is, the time-series of area-averaged SSTs in the Niño 3.4 region (hereafter EN3.4 Trenberth, 1997) and a 5-month running mean using a 0.5 K threshold to define positive or negative events. The QBO index is defined using the equatorial average [10S–10N] of zonal wind at the 70 hPa level and a ± 2 m s^{-1} threshold to define W and E phases. Given the observed and simulated relationship between the QBO and convection in the Indian Ocean found by García-Franco et al. (2022), we analyze the impact of nudging on the same index of the zonal gradient of convective activity in the Indian Ocean as a proxy of the Indian Ocean Dipole (IOD). Statistical significance in observations and individual ensemble members is diagnosed using a bootstrapping method with replacement, whereas for all ensemble-mean differences, given their relative larger sample size, standard two-sided *t*-tests are used.

2.5. Observations and Reanalysis

Observational data of precipitation and SSTs are used in this study. The Global Precipitation Climatology Project (GPCP) v2.3 (Adler et al., 2003) data set is used for precipitation analyses and the HadSST v4.0 (Kennedy et al., 2019) for SST. For the remaining diagnostics, including the zonal wind and convective precipitation we use the reanalysis ERA5 from the European Center for Medium-Range Weather Forecasts (ECMWF; Hersbach et al., 2020) downloaded at $0.75° \times 0.75°$ resolution. In all cases the data cover the period 1979–2021.

3. Results

This section first shows the impact of QBO nudging on the temperature and zonal wind variability associated with the QBO, to demonstrate that the simulations are suited for the purposes of this study. The results of the atmosphere-only and coupled experiments are presented in Sections 3.2 and 3.3, respectively. The results of these experiments are then used to investigate three of the main hypotheses for QBO tropical teleconnections in Section 3.4.

3.1. The Impact of Nudging on UTLS Variability

The impact of nudging on UTLS variability is demonstrated in Figure 2 which shows that nudging increases the UTLS temperature and zonal wind variability associated with the QBO. The AMIP/coupled nudged experiments exhibit a wider and stronger QBO signal than their corresponding control experiments and the CMIP6 experiment and more closely resemble the results from ERA5, even at subtropical latitudes where nudging was not applied.

The control-minus-nudged difference plots (Figure S2 in Supporting Information S1) illustrate that both model configurations (AMIP/coupled) have substantial biases in the strength of the QBO variability. The QBO variability is too strong in the mid-stratosphere (between 10 and 40 hPa) and too weak in the equatorial lowermost stratosphere (between 70 and 90 hPa). Note, for example, that QBO W-E temperature differences reach approximately 2.5 K in the AMIP nudged run (Figure 2b) but only 1 K in the AMIP control (Figure 2e). These results indicate that the nudging experiments has eliminated the weak bias in QBO variability of the modeled tropical UTLS region and these experiments are suitable for exploring the effect of nudging the QBO on the tropical surface.

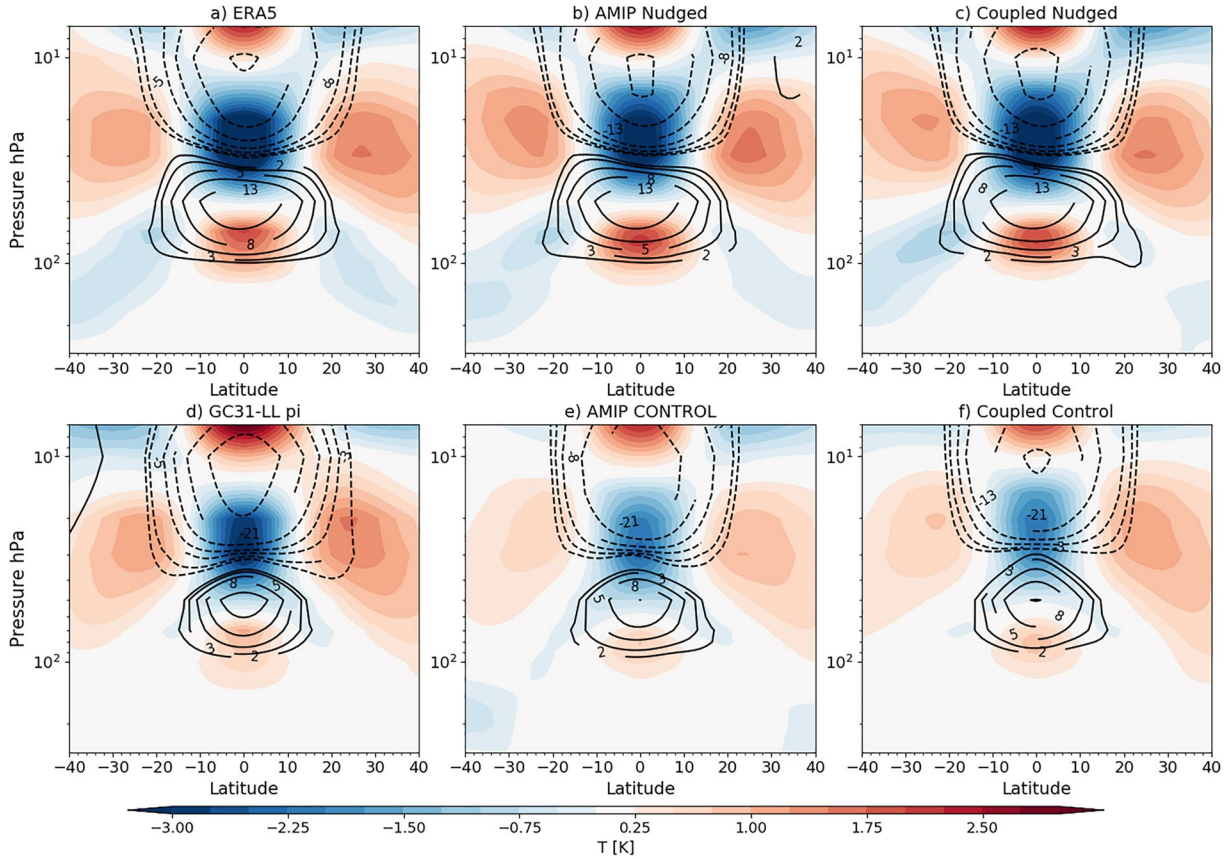

Figure 2. Latitude-height plot of the zonal-mean temperature (shading) and zonal wind (contours in m s^{-1}) QBO W-E differences in (a) ERA5, the nudged simulations in (b) AMIP and (c) coupled configurations and (d) GC3 N96-pi from CMIP6, the control simulations with no nudging in an (e) AMIP and (f) coupled configurations.

3.2. Atmosphere-Only Experiments

This section shows the results of the atmosphere-only experiments: AMIP Nudged, AMIP Control and AMIP Shifted, compared to observations (1981–2012). The annual-mean composite difference of precipitation between QBOW and E phases from the three experiments are compared with GPCP differences in Figure 3 (similar results are found for seasonal-mean composite differences—see e.g., Figure S3 in Supporting Information S1 for the December-February (DJF) results). The AMIP control experiment shows little similarity to the observations. This could be because the QBO in the control simulation is substantially underestimated in the lowermost stratosphere (as discussed in the previous section) or because the QBO mechanism involves a coupling with the ocean that is unable to operate because the SSTs are imposed.

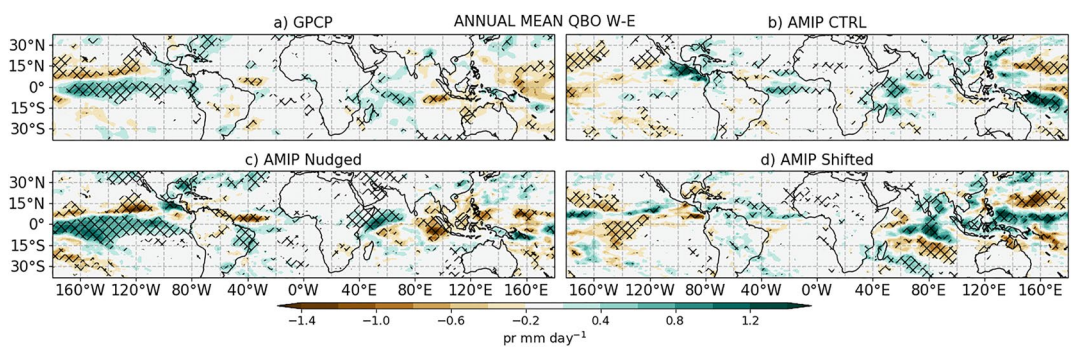

Figure 3. Annual-mean precipitation composite differences (QBO W-E in mm day^{-1}) in (a) Global Precipitation Climatology Project (GPCP), and atmosphere-only experiments: (b) AMIP CTRL, (c) AMIP Nudged and (d) AMIP Shifted.

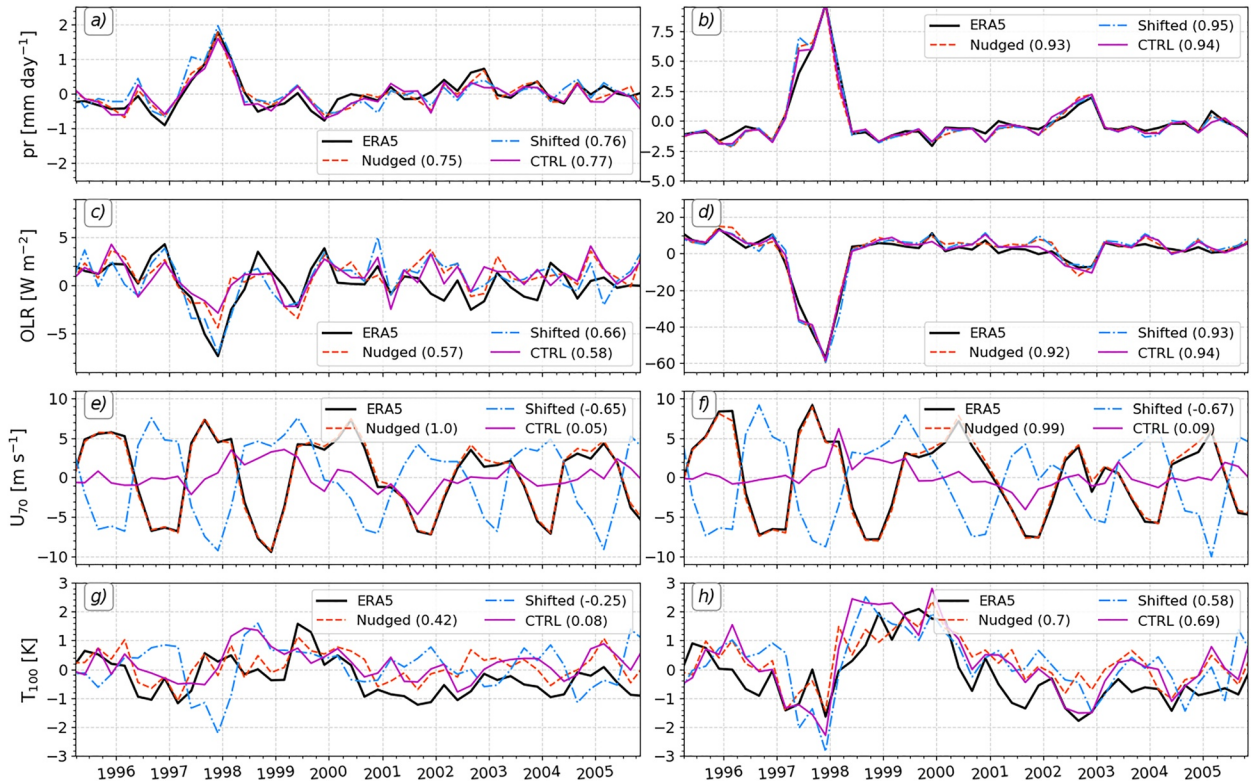

Figure 4. Time-series in the atmosphere-only experiments of (a, b) precipitation, (c, d) outgoing longwave radiation (OLR), (e, f) zonal wind at 70 hPa (U_{70}) and (g, h) air temperature at 100 hPa. The timeseries are shown for quantities averaged over the (left) zonal-mean equatorial [5°S–5°N] and (right) EN3.4 regions. For each AMIP experiment the Pearson correlation coefficient between the experiment and ERA5 is shown in the legend.

The AMIP Nudged ensemble-mean matches more closely the results of GPCP, characterized by an El Niño-like pattern in the Pacific Ocean, a weaker Atlantic ITCZ and a zonal gradient of precipitation in the Indian Ocean during QBOW compared to QBOE. This could be because the bias in the QBO amplitude has been corrected by the nudging, but it could also be because there is a QBO signal already present in the imposed observed SSTs and nudging the QBO winds means that the QBO compositing has selected the correct years. The AMIP Shifted experiment shows little similarity to the observed response. This confirms that the similarity in the precipitation differences between the observations and the AMIP Nudged experiment was not due to correcting the bias in QBO winds.

These results suggest, therefore, that the underlying SSTs are more important than the QBO winds. However, it may still be the case that tropical convection is sensitive to the QBO phase in these simulations and this effect is hidden by the strong effect of SST forcing. Time-series of the deseasonalized anomalies of multiple diagnostics averaged over all equatorial latitudes and also locally in the EN3.4 regions are shown in Figure 4. The tropical mean outgoing longwave radiation (OLR) and precipitation are not significantly affected by the nudging, confirming that convective activity is independent from the state of the QBO at 70 hPa in these simulations. The correlation coefficients of precipitation and OLR with respect to observations (a, b) are indistinguishable between experiments, both for the tropics-wide (a, c) and for the EN3.4 region (b, d).

The timeseries of the equatorial zonal mean zonal wind at 70 hPa (U_{70}; Figure 4e) shows a perfect correlation between ERA5 and the Nudged experiment, as expected. In contrast, the correlation of ERA5 with AMIP CTRL is virtually zero, because the ensemble-mean zonal wind of the CTRL collapses to near zero values. The Shifted experiment shows a negative and high correlation (0.65) with ERA5, which is not surprising, since the nudging data have been shifted by 1 year that is, approximately half a QBO cycle.

The timeseries of the near-tropopause temperature (T_{100}; Figures 4g and 4h) shows that the Nudged ensemble is correlated with ERA5 in the tropical mean. This correlation increases for the EN3.4 region in all the experiments such that the three simulations are well correlated with ERA5, although the Shifted experiment shows the lowest correlation. These results suggest the near-tropopause temperature is controlled by the QBO in the zonal-mean but by local SSTs at regional scales. In short, this section shows that in atmosphere-only experiments the nudging

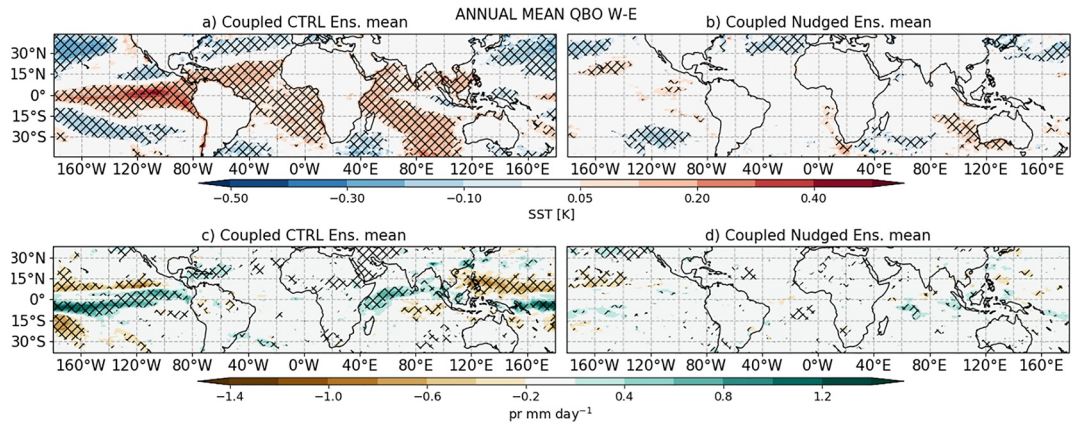

Figure 5. As in Figure 1 but for results of the (a, c) Coupled Control and (b, d) Coupled Nudged ensemble-mean (a, b) sea-surface temperature [K] and (c, d) precipitation [mm day^{-1}].

produces the expected impacts in U_{70} and the zonal-mean T_{100}, however, the nudging appears to have no made impact on the simulation of precipitation and OLR.

3.3. Coupled Experiments

This section analyses the coupled ocean-atmosphere experiments, referred to as the Coupled Nudged and the Coupled Control simulations, each of which consist of six ensemble members (see Table 1).

The annual mean QBO W-E ensemble-mean difference in tropical SSTs from the coupled control experiments (Figures 5a–5c) compares reasonably well with the results from HadSST and GC3 LL-pi (Figure 1). The precipitation response (Figure 5c) follows closely the SST patterns characterized by shifts of the ITCZ in the Pacific and Atlantic sectors and a wetter western Indian Ocean. The coupled control experiments therefore confirm the robust relationship between the QBO and tropical precipitation, characterized by stronger convection and warmer SSTs. This result is consistent with a weakened Walker circulation under QBO W as previously suggested (García-Franco et al., 2022; Hitchman et al., 2021).

However, for the Coupled Nudged ensemble-mean, the tropical SST and precipitation responses are essentially zero, although some sparse regions showing slight cooling (W-E) can be observed in the subtropics. This means that the nudging has affected the physical mechanism behind the robust statistical relationship between the tropical SSTs, precipitation and the QBO phase in the UM (García-Franco et al., 2022).

The examination of the QBO W-E differences in each of the six ensemble members in the Control and Nudged experiments (Figures S4 and S5 in Supporting Information S1) shows that the weak response in the ensemble-mean of the nudging experiments is the result of very different responses from each ensemble member. These individual responses cancel out to a large extent. In contrast, most of the control ensemble members exhibit a warming signal in the equatorial oceans, leading to the statistically significant response seen in the ensemble-mean.

One key result from García-Franco et al. (2022) was a robust relationship between the QBO and the IOD during boreal fall, September-November (SON). The QBO W-E composite differences showed positive precipitation anomalies in the western Indian Ocean and negative anomalies in the eastern Indian Ocean. Figure 6 shows that while this relationship is also found in the coupled control experiments, it is absent in the Coupled Nudged experiments. To test the significance of this result, a probability density function (PDF) of QBO W-E differences in the IOD index was constructed using 35-year blocks of the pre-industrial control experiment GC31-LL to sample internal variability within the model. The SON difference in the IOD index per QBO phase for individual ensemble members from the Control and Nudged experiments are plotted together with the PDF distribution from the GC31-LL pre-industrial control simulation (Figures 6c and 6d) to examine the likelihood that the results from the Nudged experiments occurred by chance.

The results in Figures 6c and 6d strongly suggest that the influence on the IOD is absent when nudging is applied, since some members of the Nudged ensemble show differences that are outside of the 99% range of the PDF whereas all the Control experiments show results that fall close to the median of the GC31-LL PDF. This result

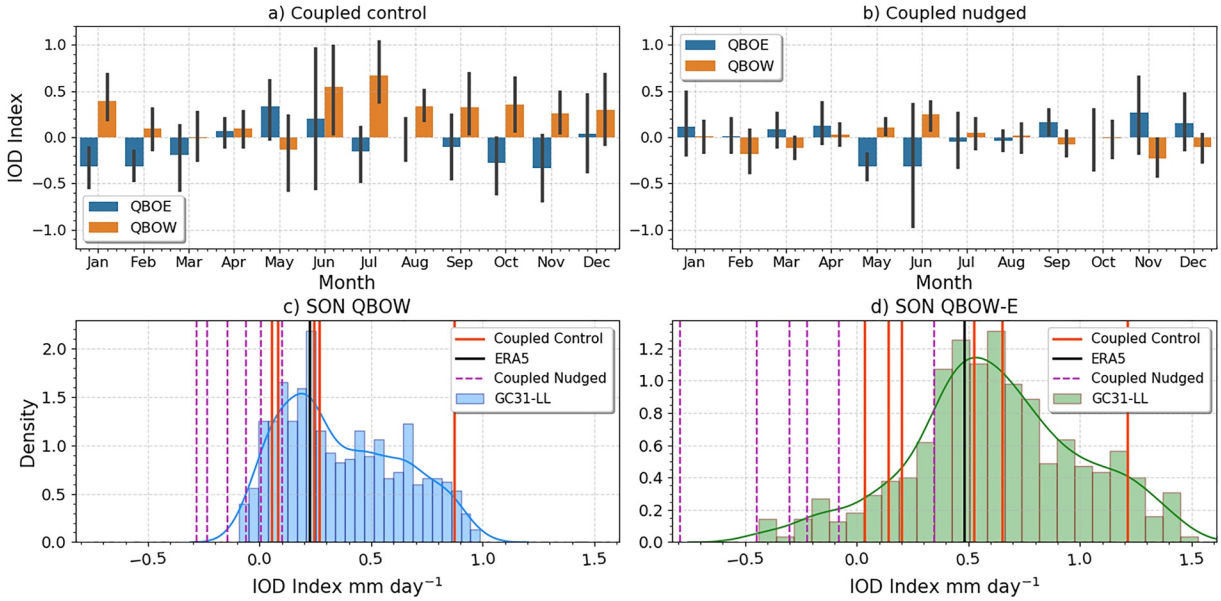

Figure 6. (a, b) Monthly-mean convective precipitation Indian Ocean Dipole (IOD) index [mm day^{-1}] in coupled (a) control and (b) nudged ensemble-means separated by quasi-biennial oscillation (QBO) phase; the error bars indicate ensemble spread. (c, d) Probability density functions (PDFs) of the IOD index in GC31-LL (see text) in SON for (c) QBOW months and (d) the QBO W-E differences. The mean values for the Coupled Control and Nudged experiments, and ERA5 are shown as vertical lines.

demonstrates that internal variability is unable to explain the differences seen in the Nudged experiment. A corresponding analysis for the EN3.4 index shows very similar results (Figure S6 in Supporting Information S1).

In summary, the results shown in this section show that the coupled control experiments in our configuration broadly reproduce those of García-Franco et al. (2022), that is, warmer SSTs and wetter conditions in the deep tropics in QBOW compared to QBOE as well as statistical links between the QBO and ENSO and the IOD. However, nudging has removed these relationships between the QBO and the tropical troposphere. Several plausible explanations for these results are discussed in Section 4. First, however, the next section evaluates three hypotheses for a QBO influence on the tropical troposphere using these experiments.

3.4. Mechanisms

Three mechanisms have been previously proposed to explain the role of the QBO in modulating aspects of tropical convection. These are referred to as the static stability mechanism, QBO-Walker circulation modulation and high-cloud radiative effects (CREs, see Section 1). This section evaluates these hypotheses through a comparison of the coupled Nudged and Control experiments.

3.4.1. The Static Stability Hypothesis

The effect of the QBO over the tropical UTLS temperature structure has been well documented (Martin, Sobel, et al., 2021; Tegtmeier et al., 2020) and is the most commonly suggested hypothesis to explain the relationships between tropical convection variability to the QBO (Collimore et al., 2003; Hitchman et al., 2021; Hu et al., 2012; J. C. K. Lee & Klingaman, 2018; Liess & Geller, 2012; Nie & Sobel, 2015). An easterly shear in the lower stratosphere induces a negative static stability anomaly in the UTLS region which increases precipitation, and the opposite is argued for a westerly shear. The UTLS static stability is defined here by the vertical temperature difference (ΔT) over the equator between 150 and 70 hPa, so that negative values indicate decreased stability. Other definitions of ΔT such as the temperature difference between 250 and 70 hPa, yield similar results to our definition.

Figure 7 shows the QBO (W-E) signal in ΔT and convective precipitation from the coupled control and nudged experiments. The spatial distribution of the ΔT differences is relatively zonally symmetric, although for ERA5 and the nudged experiments ΔT maximizes in the Eastern Pacific. The magnitude of the QBO-related variability

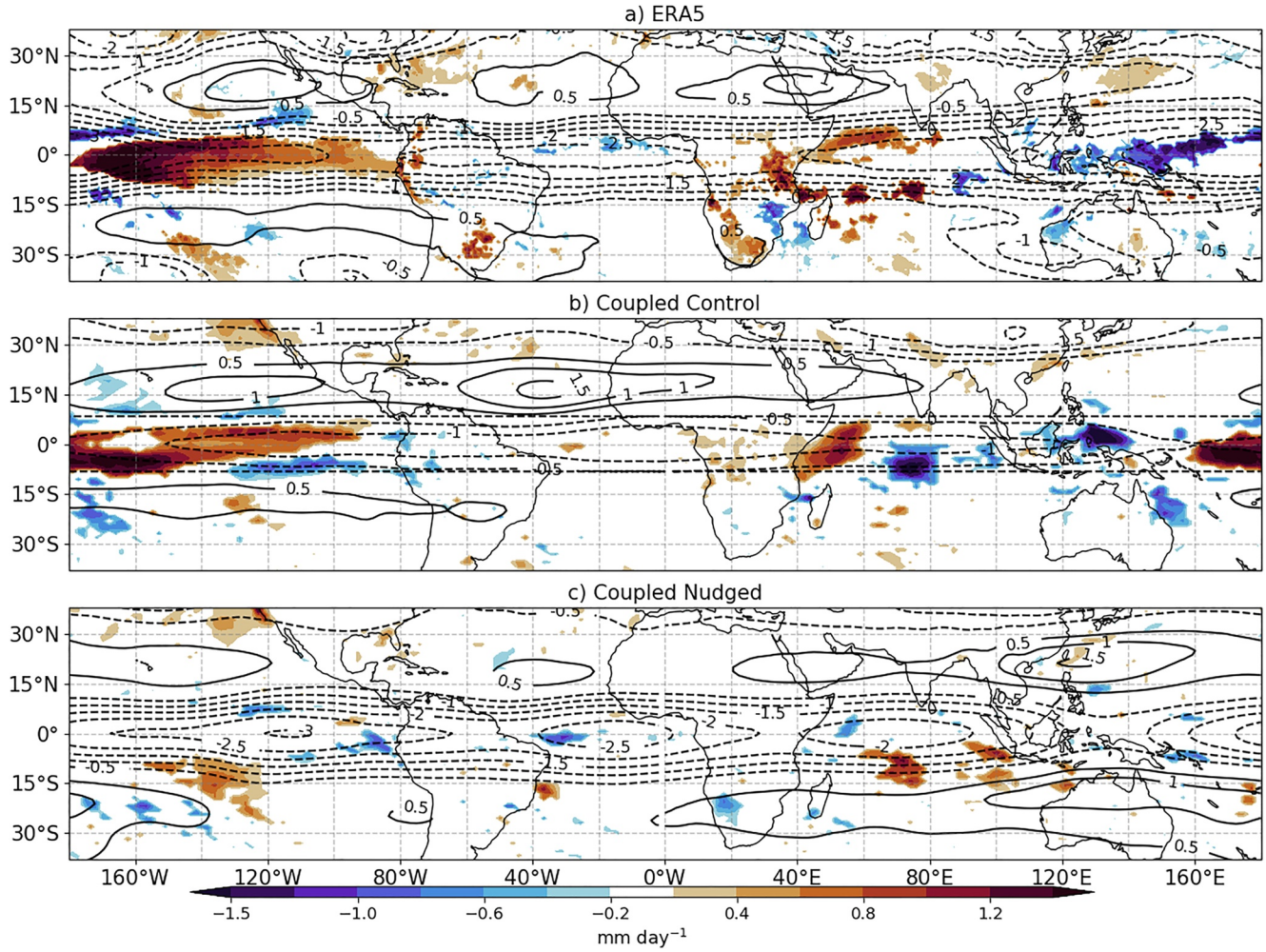

Figure 7. Convective precipitation (shading in mm day^{-1}) and upper troposphere-lower stratosphere static stability (ΔT contours in [K]) DJF composite differences (QBO W-E) in (a) ERA5 and the ensemble-mean Coupled (b) control and (c) nudged experiments. Only statistically significant differences to the 95% confidence level are plotted.

in ΔT is doubled by the nudging in the deep tropics compared to the control experiments. However, the precipitation response is not increased in the nudged experiment. The precipitation response to the QBO in models and observations is, first, not zonally symmetric and second, not co-located with the largest influence of the QBO signal on the static stability differences. The analysis of these differences in individual seasons (not shown) is consistent with this result, that is, there is no collocation of anomalies in upper level static stability with precipitation.

The potential relationship between UTLS static stability and tropical precipitation is investigated further in Figure 8. First, Figure 8a shows the scatter plot of the monthly-averaged ΔT versus Δpr in the equatorial Western Pacific [0–10N, 120–160E]; such that each point represents a month of ERA5 data. Therefore, this figure shows that these two variables have a very weak correlation. In other words, in ERA5, the temporal variability of the UTLS static stability is not related to precipitation variability in the West Pacific warm pool. The sign of the correlation coefficient (weak in any case) reverses between QBOW months and QBOE months. Similar results are found for the model simulations (not shown). This result suggests that the upper-level static stability can not explain the temporal variability of precipitation in the warm pool associated with the QBO in ERA5 or our simulations.

Next, Figure 8b shows a scatterplot of the DJF ensemble-mean QBO W-E differences of ΔT versus Δpr at each grid-point between 10S and 10N from the Coupled nudged and Coupled Control experiments. The magnitude of the negative ΔT differences is higher in the nudged experiments than in the control whereas the spread of the

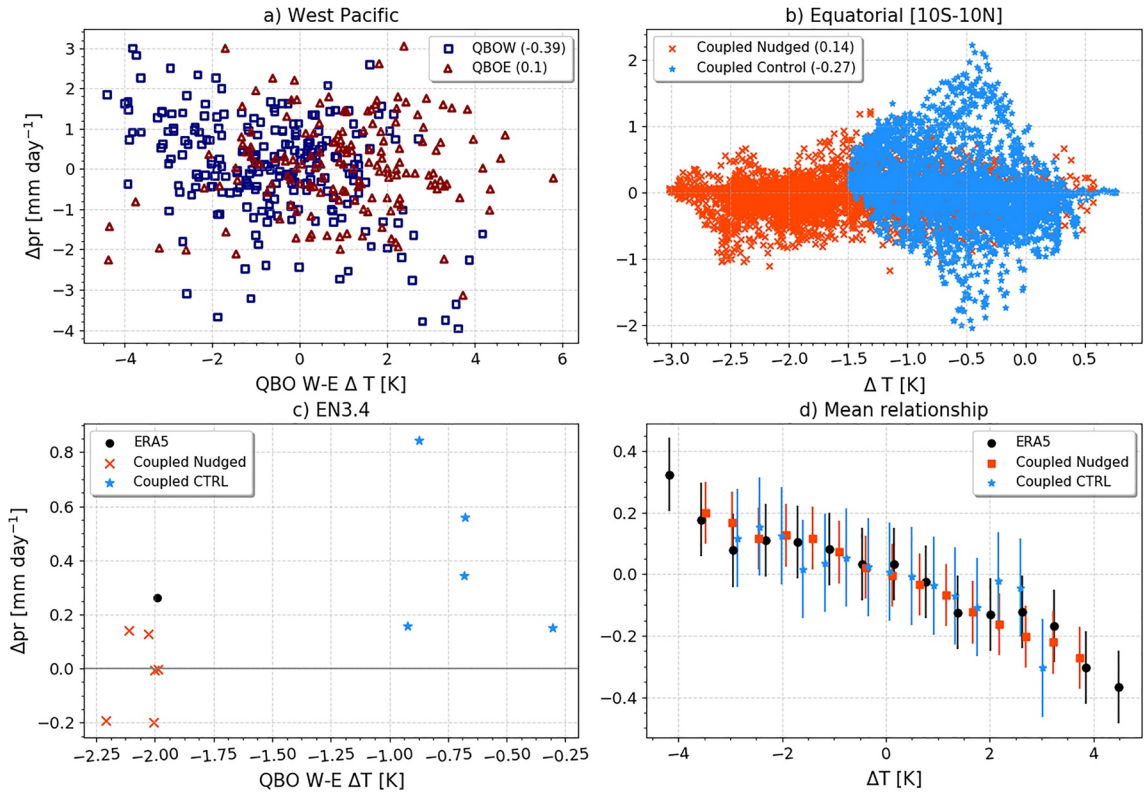

Figure 8. (a) Scatter plot of deseasonalized convective precipitation (Δpr in mm d^{-1}) versus upper troposphere-lower stratosphere static stability (ΔT in K) anomalies for the western equatorial Pacific [0–10N, 120–160E] in ERA5. Each data-point represents a month in the 1979–2021 period. (b) As in (a) but for the DJF ensemble-mean quasi-biennial oscillation (QBO) W-E differences in the equatorial latitudes [10S–10N] in the simulations, so each dot represents a grid-point. (c) Scatter plot of the annual-mean QBO W-E differences in Δpr vs. ΔT in the EN3.4 region for each ensemble member of the simulations and ERA5. (d) Mean relationship of Δpr versus ΔT computed by binning ΔT in all the grid-points at all times and computing the corresponding mean Δpr.

precipitation differences is higher in the control. This figure illustrates that the nudging increases the spread of the ΔT differences but not of precipitation. Moreover, in the control experiments, both positive and negative precipitation differences are found for similar ranges of ΔT differences. The existence of both positive and negative differences in Δpr for similar values of ΔT in the control indicates that there is no unique longitudinally coherent or zonally symmetric impact of the QBO in the model. Additionally, this plot shows that the magnitude of the precipitation differences cannot be explained by ΔT differences.

Figure 8c shows how annual mean QBO W-E differences in ΔT are related to Δpr in the Niño3.4 region for each ensemble member of the control and nudged experiments. All the coupled control ensembles show a positive precipitation difference (W-E) of up to 0.85 mm day^{-1}, even though the static stability difference (W-E) is half as strong compared to the nudged experiments. The nudged ensemble members, in contrast, simulate both positive and negative precipitation responses close to 0, indicative of no statistical relationship between ENSO and the QBO in these experiments.

Finally, Figure 8d analyses the average relationship between ΔT and Δpr. In this plot, all the monthly-mean anomalies of convective precipitation and average values of ΔT have been composited using all the grid-points at equatorial latitudes [10°S–10°N] for all the months in each simulation. This procedure pairs Δpr and ΔT taken at the same time and space coordinates. From this composite, the average Δpr anomalies were computed for equally-separated bins of ΔT (starting at the 1st percentile and up to the 99th percentile). In other words, Figure 8d shows the average precipitation anomaly for each ΔT bin. Note that in this plot, the variability of ΔT is not necessarily associated with the QBO.

The precipitation and ΔT appears to be weakly related (negatively). Relatively high UTLS static stability is associated with less precipitation and decreased static stability is associated with more precipitation, roughly a static stability anomaly of +1 K corresponds to a precipitation anomaly of −0.1 mm day^{-1}. This result would support

the main assumption of the static stability mechanism, that is, that decreased upper level static stability associated with the QBO leads to more precipitation. Figure 8d confirms that the nudging has increased ΔT variability but the nudging has increased precipitation variability only for negative ΔT values.

In summary, nudging the zonal winds has increased the ΔT variability associated with the QBO, but the time-mean composite differences (see Section 3.3) suggest that the ΔT impacts are not sufficient to produce a precipitation signal. Even though this section does not explicitly explore a potential relationship between vertical wind shear anomalies and precipitation (W. M. Gray et al., 1992; Hitchman et al., 2021), the nudging framework does increase the QBO-related variability of the UTLS vertical wind shear but no precipitation response is found which also suggests that vertical wind shear anomalies are not sufficient to simulate an impact on precipitation.

3.4.2. The Walker Circulation

Several studies have suggested a link between the QBO and the Walker circulation (Hitchman et al., 2021; Liess & Geller, 2012; Yasunari, 1989). In the free-running UM the Walker circulation is weaker under QBOW than under QBOE (García-Franco et al., 2022). Figure 9 shows the impact of nudging on the mean state and QBO-ENSO related variability of the Walker circulation. The biases in the mean-state of the Walker circulation are large in the control experiment, with differences of up to 6 m s^{-1} and 1.5 K compared to ERA5 (Figure 9a). However, nudging improves some of the zonal wind biases (b), especially in the Pacific Ocean, while also producing an impact on UTLS temperature biases (≈0.5 K).

The QBO-related Walker circulation variability appears to be affected by the nudging. In the upper troposphere, the QBO impact on the zonal wind and vertical velocities is different for nudged and control experiments (c vs. d). This difference is more obvious in the Indian Ocean sector where the control experiments suggest that the W-E response is characterized by anomalous ascent in the western sector and descent in the eastern sector, yet the nudged response is the opposite.

Regression analysis was used to investigate the interaction of ENSO, the QBO and the Walker circulation, as in García-Franco et al. (2022). Figures 9e and 9f suggest that not only are the mean-state and the QBO relationships affected but the linear relationship between ENSO and the upper branch of the Walker circulation is weakened when the nudging was applied (see e.g., 150E at 100 hPa where the temperature signal is twice as large in the control experiment). Note, however, that the lower tropospheric ENSO signal remains unchanged.

These results indicate that the effect from ENSO on to the UTLS temperature has been weakened by the nudging which suggests that the nudging may have overly constrained the upper-branch of the Walker circulation. Feedback processes between convection, the UTLS temperature and the large-scale circulation may have been reduced or modified. This possibility is discussed in Section 4.

3.4.3. The CRE Hypothesis

High clouds may play a role in the QBO tropical teleconnections through a QBO-driven modulation of the mean-state cloud fraction and/or through cloud radiative feedbacks at the convective scale (Lim & Son, 2022; Lin & Emanuel, 2023; Sun et al., 2019). Both hypotheses suggest enhanced convection under QBOE. This section uses model diagnostics such as OLR, cloud top pressure (CTP), high cloud fraction (HCF) and ice total content (QCF) to explore this hypothesis and to better understand the differences between control and nudged experiments.

The annual mean difference in HCF and QCF associated with the QBO phase (Figure 10) shows that the relationship between high clouds and the QBO is different in the nudged versus control coupled experiments. In the nudged experiments, the QBO signal is zonally symmetric, characterized by reduced HCF and QCF at equatorial regions under QBOW compared to QBOE, in agreement with previous observational and modeling studies (Sakaeda et al., 2020; Sun et al., 2019; Sweeney et al., 2023). In contrast, the differences (W-E) in the free-running control simulations show a zonally asymmetric response, for example, with a dipole of positive and negative anomalies in the Indian Ocean.

Figure 11 shows the zonal-mean differences (QBO W-E) in convective precipitation and high cloud diagnostics. First, the control experiments show a dipole response of convective precipitation in the Indian Ocean, first reported by García-Franco et al. (2022), which is also observed in OLR, HCF and QCF. In the control experiments, precipitation differences are strongly anti-correlated with OLR, as expected, and positively correlated with CTP, HCF and QCF, which illustrates that high cloud occurrence is linked to convective precipitation. However, the nudged experiments do not exhibit such clear relationships. Instead, the nudged experiments

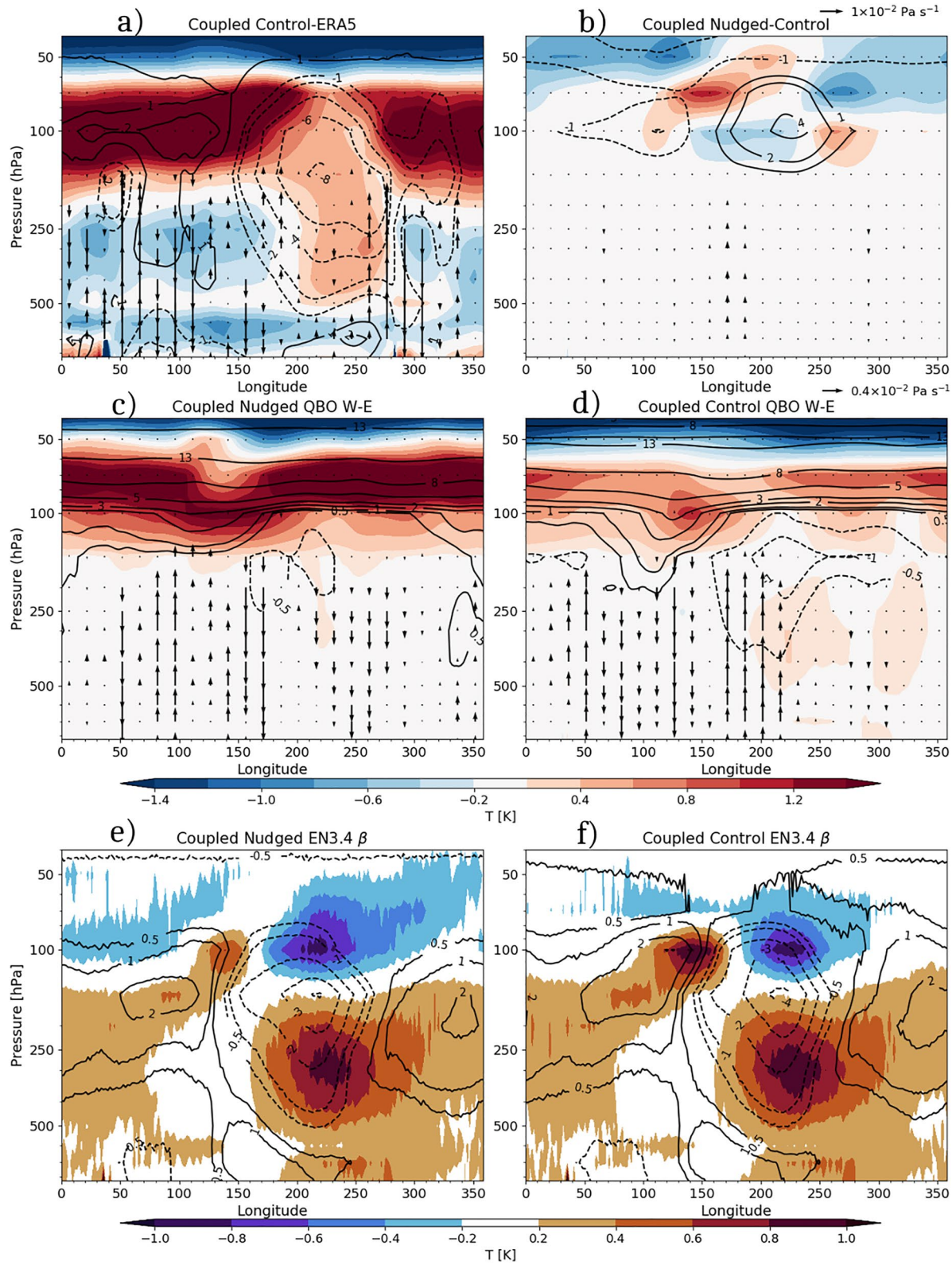

Figure 9. (a) Mean biases, diagnosed as differences between control ensemble-mean and ERA5, in the Walker circulation [10S–10N] diagnosed from the zonal mean temperature (K in shading), zonal wind (contours in m s^{-1}) and vertical velocity (vectors in Pa s^{-1}). (b) Shows the differences between Nudged and Control coupled experiments. (c)–(d) Show the QBO W-E differences for the (c) nudged and (d) control ensemble-mean. (c)–(d) Is as in (a)–(b) except that the (c)–(d) vector key is different than for (a)–(b). (e)–(f) Show the results of the regression coefficients (β) between the zonal wind (contours) and the air temperature (shading) fields with the EN3.4 index.

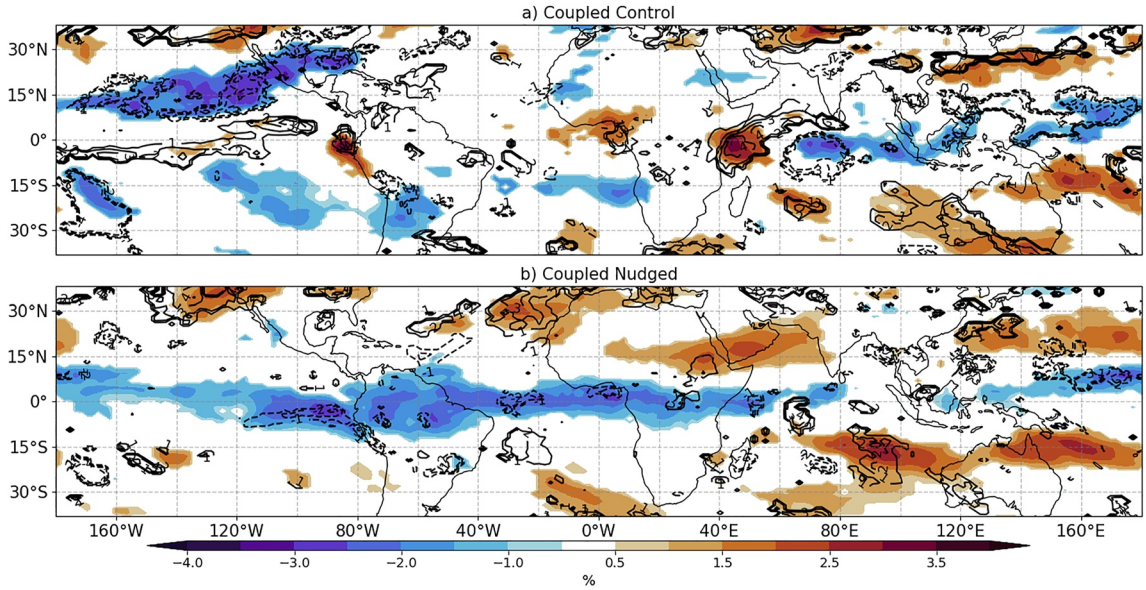

Figure 10. Annual mean differences (QBO W-E during El Niño-Southern Oscillation neutral periods) in high cloud fraction (shading in %) and ice cloud water content (contours in 10^{-2} kg m^{-2}) for Coupled Control and nudged experiments. Only statistically significant (95% confidence level) differences are plotted.

show a zonally symmetric decrease of HCF under QBOW compared to QBOE. This could suggest that without dynamical feedbacks, the QBO impact is to decrease HCF at equatorial latitudes but does not influence precipitation.

In summary, this section shows that when the stratosphere is nudged fewer high clouds are found under QBOW compared to QBOE at equatorial latitudes. However, changing the mean-state of cloud fraction is not enough to simulate a surface precipitation response. These results suggest that feedbacks between high clouds, radiation, and convection are key to the QBO influence on the troposphere and that these feedbacks have been affected by the nudging.

4. Discussion and Conclusions

Nudging experiments performed with the MOHC UM were used to explore the link between the QBO and tropical convection and precipitation. By nudging the zonal wind field in the equatorial stratosphere toward ERA5, the UM realistically reproduces the observed QBO-related variability in the zonal wind and temperature in the UTLS region. The nudging thus removed the weak QBO amplitude bias in the lower stratosphere.

In the atmosphere-only experiments, either nudged or free-running, the zonal wind in the equatorial stratosphere makes little difference to the simulation of precipitation in the UM. This result implies that any process that links the QBO to the tropical circulation within the model requires SSTs to play an active role, either driving the relationship or through SST-QBO feedbacks.

Potential QBO-SST feedbacks were investigated using coupled ocean-atmosphere experiments. In the control coupled-ocean experiments, the tropical SSTs were found to be warmer under QBOW than under QBOE, in agreement with García-Franco et al. (2022). QBO-related precipitation patterns in these experiments follow the SST patterns with wetter conditions over equatorial oceans under QBOW compared to QBOE. However, in the nudged coupled ensemble-mean, tropical SST and precipitation QBO-related differences were zero.

One possibility to explain the lack of a QBO-precipitation connection in the nudged experiments is that the simulated QBO-tropical teleconnections are the result of a bottom-up pathway which is broken when the stratosphere is nudged. It is well known that the QBO is generated by the interaction of convectively triggered waves and the stratospheric mean flow (Baldwin et al., 2001; Garfinkel et al., 2022; Geller et al., 2016; Y.-H. Kim & Chun, 2015). Since the nudging of the QBO winds toward ERA5 is applied at each grid-point, in contrast to other nudging schemes that nudged only the zonally-averaged component (Martin, Orbe, et al., 2021), the resolved

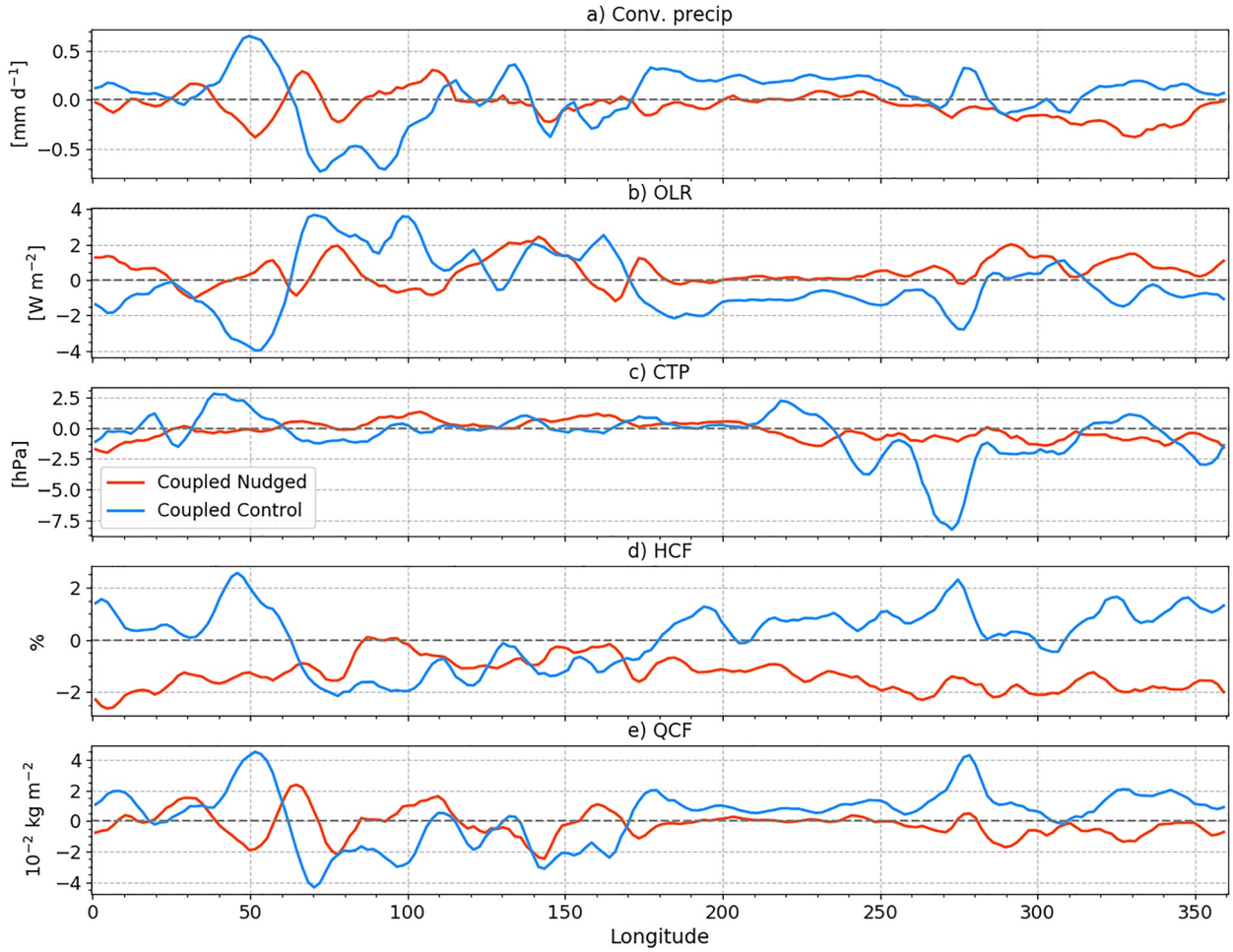

Figure 11. Zonal-mean equatorially averaged [10S–10N] annual-mean differences QBO W-E (during neutral El Niño-Southern Oscillation conditions only) of (a) convective precipitation [mm day^{-1}], (b) outgoing longwave radiation [W m^{-2}], (c) cloud top pressure [Pa], (d) high-cloud fraction [%] and (e) ice total content [10^{-2} kg m^{-2}].

wave fields just below the tropopause are likely to be inconsistent with those in the nudged region just above the tropopause, which could result in the artificially damping of waves in this height region.

To explore this hypothesis, Figure 12 shows the symmetric and anti-symmetric zonal wavenumber-frequency spectra of *u* wind at 100 hPa, following previous studies (Wheeler & Kiladis, 1999; Yang et al., 2012). Figure S7 in Supporting Information S1 shows the corresponding diagnostics at 70 hPa. At both 100 hPa and 70 hPa, the control simulation exhibits more spectral power related to the resolved Kelvin, Rossby and Mixed-Rossby Gravity waves. This evidence suggests waves may play an important role in coupling the tropical stratosphere and troposphere. Further exploration of this hypothesis, outside the scope of this study, could include nudging of the zonal-mean component of the flow, so that waves can propagate freely upward through the nudged region.

The possibility that other feedbacks are responsible for the relationships simulated in the control simulations was investigated using elements from three hypotheses that could explain QBO teleconnections in the tropics. First, this study finds that the QBO-driven variability of the UTLS static stability (Figures 7 and 8) has no robust relationship with tropical precipitation variability in the UM. Even though the QBO signal in UTLS static stability is zonally symmetric, the QBO signal in precipitation is highly asymmetric in the UM and observations. Second, although the nudged experiments doubled the UTLS static stability variability associated with the QBO, the precipitation response to the QBO phase was muted. The implication from this result is that QBO-related variability in UTLS static stability is not a sufficient process to explain the link between the QBO and tropical convection in the UM.

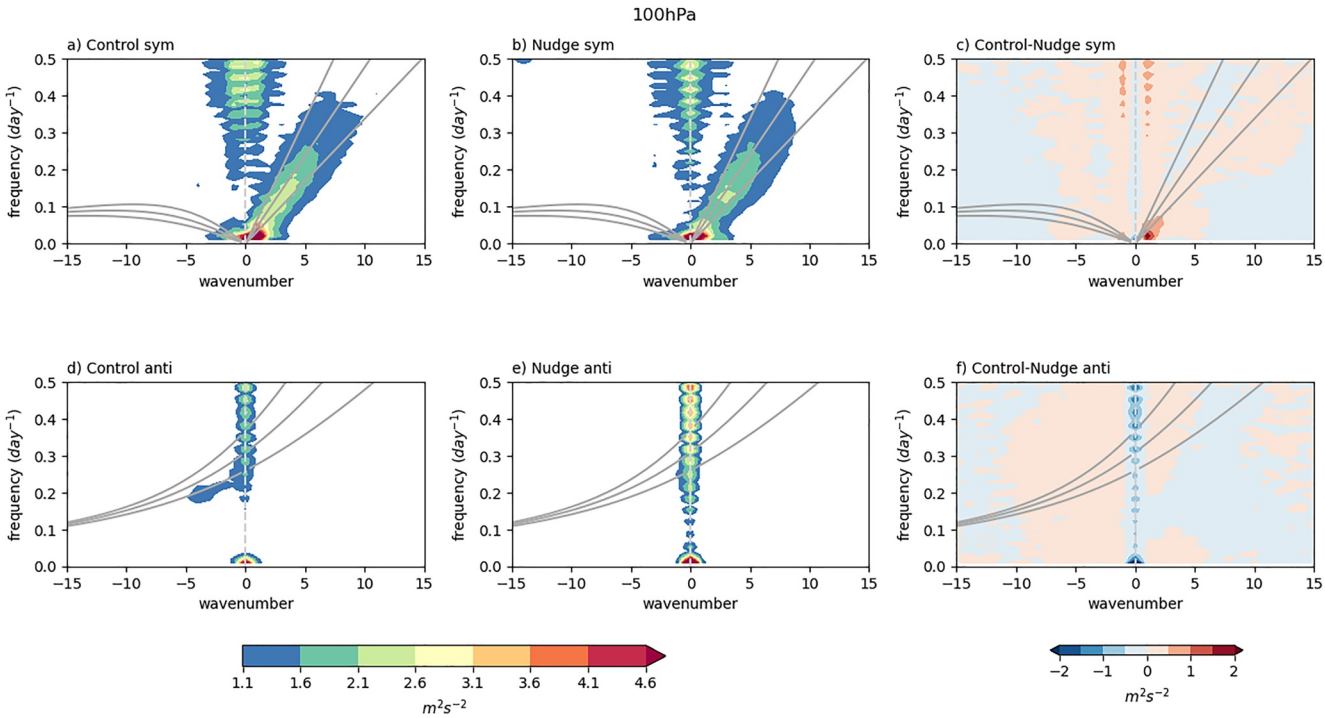

Figure 12. (a, b) Symmetric and (c, d) anti-symmetric zonal wavenumber-frequency ensemble-mean spectra of *u* wind at 100 hPa for (a, d) control and (b, e) nudged experiments. (c, f) Power spectra differences between control and nudged ensemble-mean (c) symmetric and (d) antisymmetric wavenumber-frequency 100 hPa. Dispersion curves for equivalent depths 25, 50, and 100 m are overlaid.

A second hypothesis argues that the Walker circulation is affected by the QBO, which could explain why the precipitation response in the tropics is zonally asymmetric (García-Franco et al., 2022; Hitchman et al., 2021). A weakening of the Walker circulation under QBOW compared to QBOE is diagnosed in observations, the control experiments and other versions of the UM model (García-Franco et al., 2022; Hitchman et al., 2021). However, the QBO-Walker circulation relationship was weakened when the nudging was applied to the model, likely because the nudging significantly tampered with the mean-state and variability of the upper branch of the Walker circulation decoupling the upper troposphere from the SSTs. This result suggests that the Walker circulation plays a role in amplifying local-scale effects of the QBO. This mechanism was likely muted by the nudging which has overly constrained the upper branch of the Walker circulation.

Finally, a CRE hypothesis has recently been suggested which argues that cirrus clouds play an important role in some QBO tropical teleconnections (Lin & Emanuel, 2023; Sakaeda et al., 2020; Sun et al., 2019). In the coupled control experiments, several diagnostics for high clouds were shown to be positively correlated with precipitation changes. In the nudged experiments, a robust decreased fraction of high clouds under QBOW compared to QBOE is diagnosed across equatorial regions, which agrees with some observational and modeling evidence (Lin & Emanuel, 2023; Sakaeda et al., 2020; Sun et al., 2019; Sweeney et al., 2023), but these mean-state differences in HCF are not related to precipitation. Therefore, these results suggest that the simulated QBO teleconnections require tropical stratosphere-troposphere coupling and feedbacks.

While the QBO sets the zonal-mean temperature and wind, the local conditions of clouds, convection and temperature in the tropical UTLS are heavily influenced by feedbacks at more local scales that involve the horizontal advection of clouds (Lin & Emanuel, 2023), static stability (Nie & Sobel, 2015), and upward wave propagation (Holt et al., 2022; Sakaeda et al., 2020). This means that if the QBO is linked to tropical convection in the UM through these feedback processes, our nudging setup was not the appropriate to assess or diagnose these mechanisms. Nevertheless, the findings of this study highlight the role of feedbacks, for which further improvements of the internally generated QBO by GCMs (Garfinkel et al., 2022) and of tropical convection are needed to understand the extent of stratospheric-tropospheric-coupling in the tropics.

Data Availability Statement

ERA5 reanalysis data are available from the Copernicus Climate Change Service Climate Data Store, available at ECMWF-CDS (2017). The HadSST 4.0 data set is available at Kennedy et al. (2019). The GPCP data set v2.3 is available from Adler et al. (2018). CMIP6 simulations used in this study are available from the Earth System Grid Federation of the Centre for Environmental Data Analysis (Ridley et al., 2018; WCRP, 2021).

Acknowledgments
JLGF acknowledges support from an Oxford-Richards Scholarship and a Met Office Hadley Centre PhDCASE studentship (award no. R70932/CN002). LJG and SO were supported by the United Kingdom Natural Environment Research Council and National Centre for Atmospheric Science (award nos. NE/N018028 and NE/P006779/1). We would like to thank Matthew Hitchmann and one anonymous reviewer for their constructive and helpful comments. The first author is also thankful for useful discussions of the manuscript with Isaac Held, Adam Sobel and Aodhan Sweeney.

References

Adler, R. F., Huffman, G. J., Chang, A., Ferraro, R., Xie, P.-P., Janowiak, J., et al. (2003). The version-2 global precipitation climatology project (GPCP) monthly precipitation analysis (1979–present). *Journal of Hydrometeorology*, *4*(6), 1147–1167. https://doi.org/10.1175/1525-7541(2003)004<1147:tvgpcp>2.0.co;2

Adler, R. F., Sapiano, M. R., Huffman, G. J., Wang, J.-J., Gu, G., Bolvin, D., et al. (2018). The Global Precipitation Climatology Project (GPCP) monthly analysis (new version 2.3) and a review of 2017 global precipitation [Dataset]. Atmosphere, *9*(4), 138. https://doi.org/10.7289/V56971M6

Allan, R. P. (2011). Combining satellite data and models to estimate cloud radiative effect at the surface and in the atmosphere. *Meteorological Applications*, *18*(3), 324–333. https://doi.org/10.1002/met.285

Back, S.-Y., Han, J.-Y., & Son, S.-W. (2020). Modeling evidence of QBO-MJO connection: A case study. *Geophysical Research Letters*, *47*(20), e2020GL089480. https://doi.org/10.1029/2020gl089480

Baldwin, M., Gray, L., Dunkerton, T., Hamilton, K., Haynes, P., Randel, W., et al. (2001). The quasi-biennial oscillation. *Reviews of Geophysics*, *39*(2), 179–229. https://doi.org/10.1029/1999rg000073

Bushell, A. C., Anstey, J. A., Butchart, N., Kawatani, Y., Osprey, S. M., Richter, J. H., et al. (2020). Evaluation of the quasi-biennial oscillation in global climate models for the SPARC QBO-initiative. *Quarterly Journal of the Royal Meteorological Society*, *148*(744), 1–31. https://doi.org/10.1002/qj.3765

Bushell, A. C., Butchart, N., Derbyshire, S. H., Jackson, D. R., Shutts, G. J., Vosper, S. B., & Webster, S. (2015). Parameterized gravity wave momentum fluxes from sources related to convection and large-scale precipitation processes in a global atmosphere model. *Journal of the Atmospheric Sciences*, *72*(11), 4349–4371. https://doi.org/10.1175/jas-d-15-0022.1

Collimore, C. C., Martin, D. W., Hitchman, M. H., Huesmann, A., & Waliser, D. E. (2003). On the relationship between the QBO and tropical deep convection. *Journal of Climate*, *16*(15), 2552–2568. https://doi.org/10.1175/1520-0442(2003)016<2552:otrbtq>2.0.co;2

Davis, S. M., Liang, C. K., & Rosenlof, K. H. (2013). Interannual variability of tropical tropopause layer clouds. *Geophysical Research Letters*, *40*(11), 2862–2866. https://doi.org/10.1002/grl.50512

Domeisen, D. I., Garfinkel, C. I., & Butler, A. H. (2019). The teleconnection of El Niño Southern Oscillation to the stratosphere. *Reviews of Geophysics*, *57*(1), 5–47. https://doi.org/10.1029/2018rg000596

ECMWF-CDS. (2017). ERA5: Fifth generation of ECMWF atmospheric reanalyses of the global climate [Dataset]. Copernicus Climate Change Service Climate Data Store (CDS). Retrieved from https://climate.copernicus.eu/climate-reanalysis

García-Franco, J. L., Gray, L. J., Osprey, S., Chadwick, R., & Martin, Z. (2022). The tropical route of quasi-biennial oscillation (QBO) teleconnections in a climate model. *Weather and Climate Dynamics*, *3*(3), 825–844. https://doi.org/10.5194/wcd-3-825-2022

García-Franco, J. L., Gray, L. J., & Osprey, S. (2020). The American monsoon system in HadGEM3 and UKESM1. *Weather and Climate Dynamics*, *1*(2), 349–371. https://doi.org/10.5194/wcd-1-349-2020

Garfinkel, C. I., Gerber, E. P., Shamir, O., Rao, J., Jucker, M., White, I., & Paldor, N. (2022). A QBO cookbook: Sensitivity of the quasi-biennial oscillation to resolution, resolved waves, and parameterized gravity waves. *Journal of Advances in Modeling Earth Systems*, *14*(3), e2021MS002568. https://doi.org/10.1029/2021ms002568

Garfinkel, C. I., & Hartmann, D. L. (2011). The influence of the quasi-biennial oscillation on the troposphere in winter in a hierarchy of models. Part II: Perpetual winter WACCM runs. *Journal of the Atmospheric Sciences*, *68*(9), 2026–2041. https://doi.org/10.1175/2011jas3702.1

Geller, M. A., Zhou, T., & Yuan, W. (2016). The QBO, gravity waves forced by tropical convection, and ENSO. *Journal of Geophysical Research: Atmospheres*, *121*(15), 8886–8895. https://doi.org/10.1002/2015jd024125

Giorgetta, M. A., Bengtsson, L., & Arpe, K. (1999). An investigation of QBO signals in the east Asian and Indian monsoon in GCM experiments. *Climate Dynamics*, *15*(6), 435–450. https://doi.org/10.1007/s003820050292

Gray, L., Brown, M., Knight, J., Andrews, M., Lu, H., O'Reilly, C., & Anstey, J. (2020). Forecasting extreme stratospheric polar vortex events. *Nature Communications*, *11*(1), 1–9. https://doi.org/10.1038/s41467-020-18299-7

Gray, L. J., Anstey, J. A., Kawatani, Y., Lu, H., Osprey, S., & Schenzinger, V. (2018). Surface impacts of the quasi biennial oscillation. *Atmospheric Chemistry and Physics*, *18*(11), 8227–8247. https://doi.org/10.5194/acp-18-8227-2018

Gray, W. M. (1984). Atlantic seasonal hurricane frequency. Part I: El Niño and 30 mb quasi-biennial oscillation influences. *Monthly Weather Review*, *112*(9), 1649–1668. https://doi.org/10.1175/1520-0493(1984)112<1649:ashfpi>2.0.co;2

Gray, W. M., Sheaffer, J. D., & Knaff, J. A. (1992). Influence of the stratospheric QBO on ENSO variability. *Journal of the Meteorological Society of Japan. Series II*, *70*(5), 975–995. https://doi.org/10.2151/jmsj1965.70.5_975

Harrop, B. E., & Hartmann, D. L. (2016). The role of cloud radiative heating within the atmosphere on the high cloud amount and top-of-atmosphere cloud radiative effect. *Journal of Advances in Modeling Earth Systems*, *8*(3), 1391–1410. https://doi.org/10.1002/2016ms000670

Hartmann, D. L., & Berry, S. E. (2017). The balanced radiative effect of tropical anvil clouds. *Journal of Geophysical Research: Atmospheres*, *122*(9), 5003–5020. https://doi.org/10.1002/2017jd026460

Hartmann, D. L., Holton, J. R., & Fu, Q. (2001). The heat balance of the tropical tropopause, cirrus, and stratospheric dehydration. *Geophysical Research Letters*, *28*(10), 1969–1972. https://doi.org/10.1029/2000gl012833

Haynes, P., Hitchcock, P., Hitchman, M., Yoden, S., Hendon, H., Kiladis, G., et al. (2021). The influence of the stratosphere on the tropical troposphere. *Journal of the Meteorological Society of Japan. Series II*, *99*(4), 803–845. https://doi.org/10.2151/jmsj.2021-040

Hendon, H. H., & Abhik, S. (2018). Differences in vertical structure of the Madden-Julian oscillation associated with the quasi-biennial oscillation. *Geophysical Research Letters*, *45*(9), 4419–4428. https://doi.org/10.1029/2018gl077207

Hersbach, H., Bell, B., Berrisford, P., Hirahara, S., Horányi, A., Muñoz-Sabater, J., et al. (2020). The ERA5 global reanalysis. *Quarterly Journal of the Royal Meteorological Society*, *146*(730), 1999–2049. https://doi.org/10.1002/qj.3803

Hitchman, M. H., Yoden, S., Haynes, P. H., Kumar, V., & Tegtmeier, S. (2021). An observational history of the direct influence of the stratospheric quasi-biennial oscillation on the tropical and subtropical upper troposphere and lower stratosphere. *Journal of the Meteorological Society of Japan. Series II*, *99*(2), 239–267. https://doi.org/10.2151/jmsj.2021-012

Holt, L. A., Lott, F., Garcia, R. R., Kiladis, G. N., Cheng, Y.-M., Anstey, J. A., et al. (2022). An evaluation of tropical waves and wave forcing of the QBO in the QBOi models. *Quarterly Journal of the Royal Meteorological Society*, *148*(744), 1541–1567. https://doi.org/10.1002/qj.3827

Hong, Y., Liu, G., & Li, J.-L. (2016). Assessing the radiative effects of global ice clouds based on CloudSat and CALIPSO measurements. *Journal of Climate*, *29*(21), 7651–7674. https://doi.org/10.1175/jcli-d-15-0799.1

Hu, Z.-Z., Huang, B., Kinter, J. L., Wu, Z., & Kumar, A. (2012). Connection of the stratospheric QBO with global atmospheric general circulation and tropical SST. Part II: Interdecadal variations. *Climate Dynamics*, *38*(1), 25–43. https://doi.org/10.1007/s00382-011-1073-6

Kennedy, J. J., Rayner, N., Atkinson, C., & Killick, R. (2019). An ensemble data set of sea surface temperature change from 1850: The Met Office Hadley Centre HadSST. 4.0. 0.0 data set [Dataset]. Journal of Geophysical Research: Atmospheres, *124*(14), 7719–7763. Retrieved from https://www.metoffice.gov.uk/hadobs/hadsst4/data/download.html. https://doi.org/10.1029/2018JD029867

Kim, H., Caron, J. M., Richter, J. H., & Simpson, I. R. (2020). The lack of QBO-MJO connection in CMIP6 models. *Geophysical Research Letters*, *47*(11), e2020GL087295. https://doi.org/10.1029/2020GL087295

Kim, Y.-H., & Chun, H.-Y. (2015). Contributions of equatorial wave modes and parameterized gravity waves to the tropical QBO in HadGEM2. *Journal of Geophysical Research: Atmospheres*, *120*(3), 1065–1090. https://doi.org/10.1002/2014jd022174

Lee, J. C. K., & Klingaman, N. P. (2018). The effect of the quasi-biennial oscillation on the Madden–Julian oscillation in the Met Office Unified Model Global Ocean Mixed Layer configuration. *Atmospheric Science Letters*, *19*(5), e816. https://doi.org/10.1002/asl.816

Lee, J.-H., Kang, M.-J., & Chun, H.-Y. (2019). Differences in the tropical convective activities at the opposite phases of the quasi-biennial oscillation. *Asia-Pacific Journal of Atmospheric Sciences*, *55*(3), 317–336. https://doi.org/10.1007/s13143-018-0096-x

Liess, S., & Geller, M. A. (2012). On the relationship between QBO and distribution of tropical deep convection. *Journal of Geophysical Research*, *117*(D3), D03108. https://doi.org/10.1029/2011jd016317

Lim, Y., & Son, S.-W. (2022). QBO wind influence on MJO-induced temperature anomalies in the upper troposphere and lower stratosphere in an idealized model. *Journal of the Atmospheric Sciences*, *79*(9), 2219–2228. https://doi.org/10.1175/jas-d-21-0296.1

Lin, J., & Emanuel, K. (2023). Stratospheric modulation of the MJO through cirrus cloud feedbacks. *Journal of the Atmospheric Sciences*, *80*(1), 273–299.

Martin, Z., Orbe, C., Wang, S., & Sobel, A. (2021). The MJO–QBO relationship in a GCM with stratospheric nudging. *Journal of Climate*, *34*(11), 4603–4624. https://doi.org/10.1175/jcli-d-20-0636.1

Martin, Z., Sobel, A., Butler, A., & Wang, S. (2021). Variability in QBO temperature anomalies on annual and decadal time scales. *Journal of Climate*, *34*(2), 589–605. https://doi.org/10.1175/jcli-d-20-0287.1

Martin, Z., Son, S.-W., Butler, A., Hendon, H., Kim, H., Sobel, A., et al. (2021). The influence of the quasi-biennial oscillation on the Madden–Julian oscillation. *Nature Reviews Earth & Environment*, *2*(7), 477–489.

Martin, Z., Wang, S., Nie, J., & Sobel, A. (2019). The impact of the QBO on MJO convection in cloud-resolving simulations. *Journal of the Atmospheric Sciences*, *76*(3), 669–688. https://doi.org/10.1175/jas-d-18-0179.1

Menary, M. B., Kuhlbrodt, T., Ridley, J., Andrews, M. B., Dimdore-Miles, O. B., Deshayes, J., et al. (2018). Preindustrial control simulations with HadGEM3-GC3. 1 for CMIP6. *Journal of Advances in Modeling Earth Systems*, *10*(12), 3049–3075. https://doi.org/10.1029/2018ms001495

Needham, M. R., & Randall, D. A. (2021). Linking atmospheric cloud radiative effects and tropical precipitation. *Geophysical Research Letters*, *48*(14), e2021GL094004. https://doi.org/10.1029/2021gl094004

Nie, J., & Sobel, A. H. (2015). Responses of tropical deep convection to the QBO: Cloud-resolving simulations. *Journal of the Atmospheric Sciences*, *72*(9), 3625–3638. https://doi.org/10.1175/jas-d-15-0035.1

Politowicz, P. A., & Hitchman, M. H. (1997). Exploring the effects of forcing quasi-biennial oscillations in a two-dimensional model. *Journal of Geophysical Research*, *102*(D14), 16481–16497. https://doi.org/10.1029/97jd00693

Rädel, G., Mauritsen, T., Stevens, B., Dommenget, D., Matei, D., Bellomo, K., & Clement, A. (2016). Amplification of El Nino by cloud longwave coupling to atmospheric circulation. *Nature Geoscience*, *9*(2), 106–110. https://doi.org/10.1038/ngeo2630

Rao, J., Garfinkel, C. I., & White, I. P. (2020). How does the quasi-biennial oscillation affect the boreal winter tropospheric circulation in CMIP5/6 models? *Journal of Climate*, *33*(20), 8975–8996. https://doi.org/10.1175/jcli-d-20-0024.1

Richter, J. H., Anstey, J. A., Butchart, N., Kawatani, Y., Meehl, G. A., Osprey, S., & Simpson, I. R. (2020). Progress in simulating the quasi-biennial oscillation in CMIP models. *Journal of Geophysical Research: Atmospheres*, *125*(8), e2019JD032362. https://doi.org/10.1029/2019JD032362

Ridley, J., Menary, M., Kuhlbrodt, T., Andrews, M., & Andrews, T. (2018). MOHC HadGEM3-GC31-LL model output prepared for CMIP6 CMIP piControl [Dataset]. Earth System Grid Federation. https://doi.org/10.22033/ESGF/CMIP6.6294

Sakaeda, N., Dias, J., & Kiladis, G. N. (2020). The unique characteristics and potential mechanisms of the MJO-QBO relationship. *Journal of Geophysical Research: Atmospheres*, *125*(17), e2020JD033196. https://doi.org/10.1029/2020jd033196

Schenzinger, V., Osprey, S., Gray, L., & Butchart, N. (2017). Defining metrics of the quasi-biennial oscillation in global climate models. *Geoscientific Model Development*, *10*(6), 2157–2168. https://doi.org/10.5194/gmd-10-2157-2017

Schirber, S. (2015). Influence of ENSO on the QBO: Results from an ensemble of idealized simulations. *Journal of Geophysical Research: Atmospheres*, *120*(3), 1109–1122. https://doi.org/10.1002/2014jd022460

Serva, F., Anstey, J. A., Bushell, A. C., Butchart, N., Cagnazzo, C., Gray, L., et al. (2022). The impact of the QBO on the region of the tropical tropopause in QBOi models: Present-day simulations. *Quarterly Journal of the Royal Meteorological Society*, *148*(745), 1945–1964. https://doi.org/10.1002/qj.4287

Son, S.-W., Lim, Y., Yoo, C., Hendon, H. H., & Kim, J. (2017). Stratospheric control of the Madden–Julian oscillation. *Journal of Climate*, *30*(6), 1909–1922. https://doi.org/10.1175/jcli-d-16-0620.1

Storkey, D., Blaker, A. T., Mathiot, P., Megann, A., Aksenov, Y., Blockley, E. W., et al. (2018). UK Global Ocean GO6 and GO7: A traceable hierarchy of model resolutions. *Geoscientific Model Development*, *11*(8), 3187–3213. https://doi.org/10.5194/gmd-11-3187-2018

Sun, L., Wang, H., & Liu, F. (2019). Combined effect of the QBO and ENSO on the MJO. *Atmospheric and Oceanic Science Letters*, *12*(3), 170–176. https://doi.org/10.1080/16742834.2019.1588064

Sweeney, A., Fu, Q., Pahlavan, H. A., & Haynes, P. (2023). Seasonality of the QBO impact on equatorial clouds. *Journal of Geophysical Research: Atmospheres*, *128*(7), e2022JD037737. https://doi.org/10.1029/2022JD037737

Taguchi, M. (2010). Observed connection of the stratospheric quasi-biennial oscillation with El Niño–Southern Oscillation in radiosonde data. *Journal of Geophysical Research*, *115*(D18), D18120. https://doi.org/10.1029/2010jd014325

Tegtmeier, S., Anstey, J., Davis, S., Ivanciu, I., Jia, Y., McPhee, D., & Pilch Kedzierski, R. (2020). Zonal asymmetry of the QBO temperature signal in the tropical tropopause region. *Geophysical Research Letters*, *47*(24), e2020GL089533. https://doi.org/10.1029/2020GL089533

Telford, P., Braesicke, P., Morgenstern, O., & Pyle, J. (2008). Description and assessment of a nudged version of the new dynamics unified model. *Atmospheric Chemistry and Physics*, *8*(6), 1701–1712. https://doi.org/10.5194/acp-8-1701-2008

Trenberth, K. E. (1997). The definition of El Nino. *Bulletin of the American Meteorological Society*, *78*(12), 2771–2778. https://doi.org/10.1175/1520-0477(1997)078<2771:tdoeno>2.0.co;2

Tseng, H.-H., & Fu, Q. (2017). Temperature control of the variability of tropical tropopause layer cirrus clouds. *Journal of Geophysical Research: Atmospheres*, *122*(20), 11–062. https://doi.org/10.1002/2017jd027093

Walters, D., Boutle, I., Brooks, M., Melvin, T., Stratton, R., Vosper, S., et al. (2019). The Met Office Unified Model global atmosphere 7.0/7.1 and JULES global land 7.0 configurations. *Geoscientific Model Development*, *12*(5), 1909–1963. https://doi.org/10.5194/gmd-12-1909-2019

WCRP. (2021). World climate research programme (WCRP): Coupled model intercomparison project (phase 6) [Dataset]. Retrieved from https://esgf-index1.ceda.ac.uk/projects/cmip6-ceda/

Wheeler, M., & Kiladis, G. N. (1999). Convectively coupled equatorial waves: Analysis of clouds and temperature in the wavenumber–frequency domain. *Journal of the Atmospheric Sciences*, *56*(3), 374–399. https://doi.org/10.1175/1520-0469(1999)056<0374:ccewao>2.0.co;2

Williams, K. D., Copsey, D., Blockley, E. W., Bodas-Salcedo, A., Calvert, D., Comer, R., et al. (2018). The Met Office global coupled model 3.0 and 3.1 (GC3. 0 and GC3. 1) configurations. *Journal of Advances in Modeling Earth Systems*, *10*(2), 357–380. https://doi.org/10.1002/2017ms001115

Yang, G.-Y., Hoskins, B., & Gray, L. (2012). The influence of the QBO on the propagation of equatorial waves into the stratosphere. *Journal of the Atmospheric Sciences*, *69*(10), 2959–2982. https://doi.org/10.1175/jas-d-11-0342.1

Yasunari, T. (1989). A possible link of the QBOs between the stratosphere, troposphere and sea surface temperature in the tropics. *Journal of the Meteorological Society of Japan. Series II*, *67*(3), 483–493. https://doi.org/10.2151/jmsj1965.67.3_483

Yoo, C., & Son, S.-W. (2016). Modulation of the boreal wintertime Madden-Julian oscillation by the stratospheric quasi-biennial oscillation. *Geophysical Research Letters*, *43*(3), 1392–1398. https://doi.org/10.1002/2016gl067762

Zhang, C., & Zhang, B. (2018). QBO-MJO connection. *Journal of Geophysical Research: Atmospheres*, *123*(6), 2957–2967. https://doi.org/10.1002/2017jd028171